ELSEVIER

Ceramics International 33 (2007) 405–412

CERAMICS INTERNATIONAL

www.elsevier.com/locate/ceramint

Monitoring of transformations in bentonite after NaOH-TMA treatment

M. Vlasova [a,*], I. Leon [a], Y. Enríquez Méndez [a], G. Dominguez-Patiño [a], M. Kakazey [a], M. Dominguez-Patiño [a], M.V. Nikolic [b], M.M. Ristic [c]

[a] *The Autonomous University of the State of Morelos, Av. Universidad, 1001, Cuernavaca, Mexico*
[b] *Center for Multidisciplinary Studies of the University of Belgrade, Belgrade, Serbia and Montenegro*
[c] *Institute of Technical Sciences of the Serbian Academy of Sciences and Arts, Belgrade, Serbia and Montenegro*

Received 29 July 2005; received in revised form 11 August 2005; accepted 23 September 2005
Available online 18 January 2006

Abstract

Semi-quantitative methods of X-ray diffraction and FTIR-spectroscopy, accompanied by electron microscopy, X-ray microanalysis and others were used to monitor structural-phase reorganizations occurring in a smectite–gypsum mixture (bentonite) subjected to NaOH treatment with the subsequent addition of quaternary ammonium salt (TMA) in conditions of water deficiency. The interaction of bentonite with NaOH breaks up large bentonite aggregates, saturates smectite with Na cations, and yields $Ca(OH)_2$. The addition of TMA is accompanied by its penetration into the interlayer space and adsorption on the surface.

Keywords: Bentonite; NaOH; Quaternary ammonium salt; Saturation; Monitoring

1. Introduction

Bentonite clays consisting mainly of montmorillonite are widely utilized in various engineering applications. After special treatment-modification bentonite is rendered a good adsorbent material [1–4]. Treatment by inorganic acids and alkalis and saturation of montmorillonite by polyvalent metal cations is the method most widely used to modify the sorptive properties of bentonite clays [5–11]. On the other hand, it is known that montmorillonite can be rendered organophilic after saturation by organic cations [12–17].

Practically in all work up to now basic attention has been given to processes causing reorganization of montmorillonite. However, bentonites contain other minerals such as quartz, gypsum, calcite, etc. For various chemical treatments accessory phases (accessory minerals) can participate in the formation of new compounds and influence processes of structural reorganization of smectite. But usually only dissolution of accessory minerals during treatment with acids and alkalis is mentioned [8,10,14].

The purpose of this work is monitoring of phase and structural transformations in bentonite and clarification of the role of accessory phases during treatment by alkaline solutions. Alkali treatment of bentonite was carried out in conditions of water deficiency so as to avoid fast interaction of NaOH with accessory phases and smectite. Conditions of water deficiency were maintained in the stage of the introduction of quaternary ammine.

Whereas the structural-phase changes in conditions of water deficiency can be insignificant, a visual qualitative estimation of X-ray line amplitudes on diffractograms and the line (0 0 1) of montmorillonite can be insufficient for a proper analysis. In this case semi-quantitative X-ray phase and Infrared analyses are the most widespread and informative. In the first method an external or internal standard is used. In the second case a fixed ratio of components (researched substance and inert thinner) is used. The specified semi-quantitative methods of research will enable monitoring of structural-phase transformations, which occur due to various influences on a clay mineral.

2. Materials and methods

A local manufacturer (Mexico) supplied the bentonite. It had the following chemical composition (in wt.%): SiO_2 (59.0),

* Corresponding author. Tel.: +52 777 329 70 84; fax: +52 777 329 70 84.
E-mail address: kakazey@hotmail.com (M. Vlasova).

0272-8842/$32.00
doi:10.1016/j.ceramint.2005.09.024

Al_2O_3 (21.0), Fe_2O_3 (9.0), MgO (3.3), CaO (3.5), Na_2O (0.5), K_2O (0.8). The quaternary ammonium compound (tetramethylammonium chloride, marked as TMA) was obtained from Sigma Chemical. All other reagents were analytical grade ones from the firm Baker.

A series of activated samples was prepared. In order to slow down the interaction of alkali with bentonite 2 ml of a NaOH solution of with pH 12 was added to every sample of initial bentonite (series **a**) (2 g with humidity 30%). The samples were then dried at 25 °C until evaporation of water (series **b**). Bentonite activated in such a way was not washed by water. In the next stage 1.2 g of TMA dissolved in 3 ml of water was added to samples of series **b**, which were then dried at 25 °C until evaporation of water (series **c**). Liquid probes were taken from five samples of series **b** and **c** and then evaporated for determination of the phase composition of reaction products. The general preparation scheme is given in Fig. 1.

For carrying out experimental research of series **b–c** the samples were subsequently dried at 70 °C for 30 min.

Mineralogical changes in bentonite after different types of treatment were investigated by X-ray diffraction (Siemens D-500 X-ray diffractometer, Cu Kα radiation). The change of diffraction line intensity (the area under the diffraction line) of various crystalline phases was estimated relative to the line of cristobalite ($d = 0.405$ nm), which was chosen as the internal standard. If for a qualitative X-ray analysis a recording of diffractograms (Fig. 2) was carried out with a speed of 2°/min, then for correct estimation of the square under a chosen diffraction line was 0.5°/min. Results of such measurements are submitted as histograms. Let us note, that for partial overlapping of lines belonging to various phases, a mathematical operation of division into Gauss lines was carried out. The relative content of smectite was estimated by the line with $d \cong 0.45$ nm, gypsum with $d \cong 0.756$ nm and quartz $d \cong 0.334$ nm. As the line of cristobalite was chosen as an internal standard, it was necessary to establish that the conditions of NaOH treatment did not change the content of cristobalite. With this purpose cristobalite crystals with dispersiveness ∼1 μm were subjected to similar treatment.

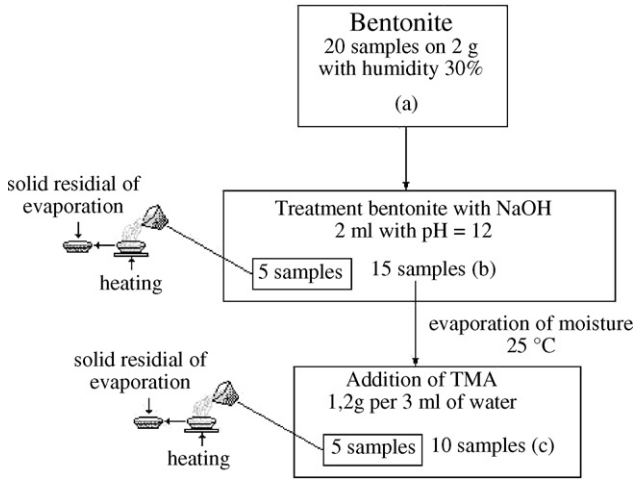

Fig. 1. General schema of sample preparation.

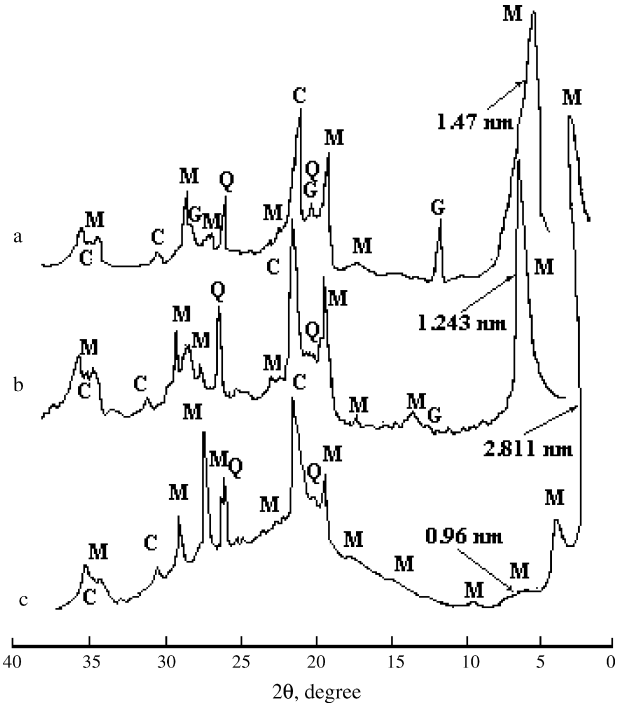

Fig. 2. X-ray difractograms of initial bentonite clay (a); after introduction of NaOH (b); after introduction of TMA in samples **b** (c). M is smectite, G is gypsum, C is cristobalite and Q is quartz.

It was established that the weight of the sample after careful washing did not change. This means that an interaction between the alkali and cristobalite without heating did not occur.

FTIR-spectra of samples were obtained on a Brucker V22 FTIR spectrometer. Measured samples contained a fixed amount of clay and KBr (2 mg of clay and 300 mg of chemically pure KBr) and were prepared as plates 8 mm × 40 mm. For a correct estimation of the square under absorption curves and comparison with various samples (semi-quantitative analysis) bentonite with an aggregate dispersity ∼10 μm was used for the preparation of plates (KBr: bentonite). The time of spectra integration was 5 min. The results of such measurements are submitted as histograms. In the case of superposition of FTIR absorption lines of various minerals a computer simulation of superimposed standard spectra of various intensities was carried out and compared with experimental spectra. Experimental spectra given in Fig. 3 were recorded with the integration time of 1 min.

Morphological studies of bentonite before and after activation were carried out using Scanning Electron Microscopy (SEM) on a Jeol JSM 6400 device and Atomic Force Microscopy (AFM) measurements were performed on a Nanoscope IV, Digital Instruments device. Height and phase recording regimes were used.

The specific surface area of the reacted products was measured using adsorption of nitrogen gas (BET method) on a Quantasorb Jr. differential flux analyzer.

X-ray microanalysis of samples was performed on a ‘‘Comebax SX50’’ unit.

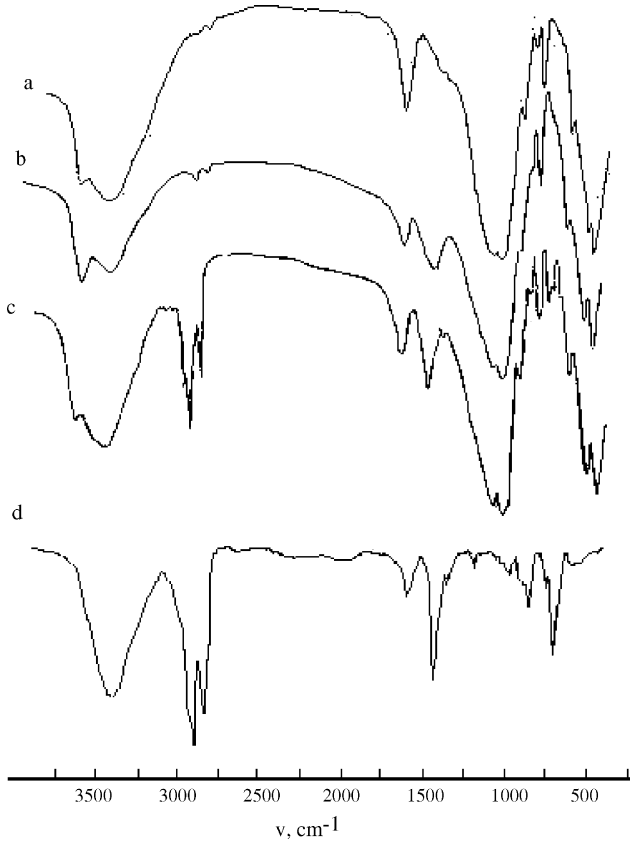

Fig. 3. FTIR-spectra of absorption in a sample of initial bentonite clay (a); after addition of NaOH (b); after addition of TMA in samples **b** (c); FTIR-spectra of absorption of TMA (d).

The cation exchange capacity (CEC) of bentonite samples was measured by $MgCl_2$ saturation and the subsequent displacement by $CaCl_2$ [18,19].

pH monitoring was performed on a ''KL-008'' pH-meter with a calomel electrode.

In view of the specificity of sample preparation (without water washing) the results obtained using BET and CEC methods reflect only the tendency of the change of clay properties and have an auxiliary character.

3. Experimental results

3.1. Bentonite (series *a*)

The X-ray analysis has shown that besides smectite, bentonite samples contain gypsum, cristobalite and quartz (Fig. 2a).

The FTIR-spectrum of bentonite clay showed a set of bands, which are characteristic for smectite (Table 1 and Fig. 3a).

SEM and AFM data shows (Figs. 4a and 5) that particles of smectite are organized in aggregates. Aggregates include various accessory phases. In Fig. 5b they have various colours. According to X-ray data it is possible to attribute inclusions to congestions of gypsum, cristobalite and quartz. The specific surface area is 9 m^2/g. CEC is 66 meq/100 g, while the pH of the bentonite is 8.

3.2. Bentonite activation (series *b*)

After addition of NaOH in samples of series **a**, the pH of the system increased up to 12. According to the X-ray data treatment of bentonite clay with NaOH is accompanied by reduction of the smectite content and disappearance of gypsum (Fig. 6). The increase of halo intensity in the region 20–30° corresponding to the increase of the amorphous phase content is marked (see Figs. 2a, b and 6). The value of $d_{(001)}$ for smectite is decreased from 1.47 to 1.243 nm. Reduction of the smectite content and disappearance of gypsum denote the occurrence of a chemical interaction of the specified components with NaOH.

Changes of FTIR-spectrum after addition of NaOH into bentonite consist in the following. The intensities of absorption bands attributed to interlayer water (3456 and 1637 cm^{-1}) decrease (Fig. 3a and b). This process is similar to the dehydration of bentonite.

The intensity of absorption bands of AlAlOH- and AlMgOH-bonds (915 and 842 cm^{-1}, respectively) decreases. The intensity of the absorption band at 794.6 cm^{-1} attributed to Si–O bonds increases insignificantly (Fig. 7). It denotes destruction of Si–O–Al, both Si–O–Mg bonds and formation of SiO_2. At the same

Table 1
FTIR-bands of absorption in investigated samples

Sample	ν, cm^{-1}								
Bentonite (**a**)	3620.6 **3448.1**m	2911w 2838.5w	1637m	1380w	1191.7sh 1103sh **1036.3**st	915.2m	842.5w	795.8m	623.3 518.8st **466.8**st
Bentonite with NaOH (**b**)	3627.4 **3451.7**m	2906.2w 2812.5w	1642.7w	1452.1w	1093.7sh **1034.3**st	921.5m		793.8m	625.8 520.8st **466.4**st
Bentonite **b** with TMA (**c**)	3609.4 **3451.7**m	2926.1m* 2851.4m*	1637.3w	1466w	1090.7sh **1036**st	915.1w 890.6sh*	844w	792.8w	728.6w*624.8 703.9w*519st **463.7**st
TMA	**3434**st	2924.9st 2854.5st	1627.4w	1463.9st 1359.4sh 1296.8sh	1218.3w	1031.2sh 1002.4w	937.5sh 879.4w	781.2sh 729.5m	625w 541.8sh

Note: st: strong; m: middle; w:– weak; sh: shoulder; (*) presence of organic molecule bands. The bold font marks the basic band, on which the bands given in the column settle down.

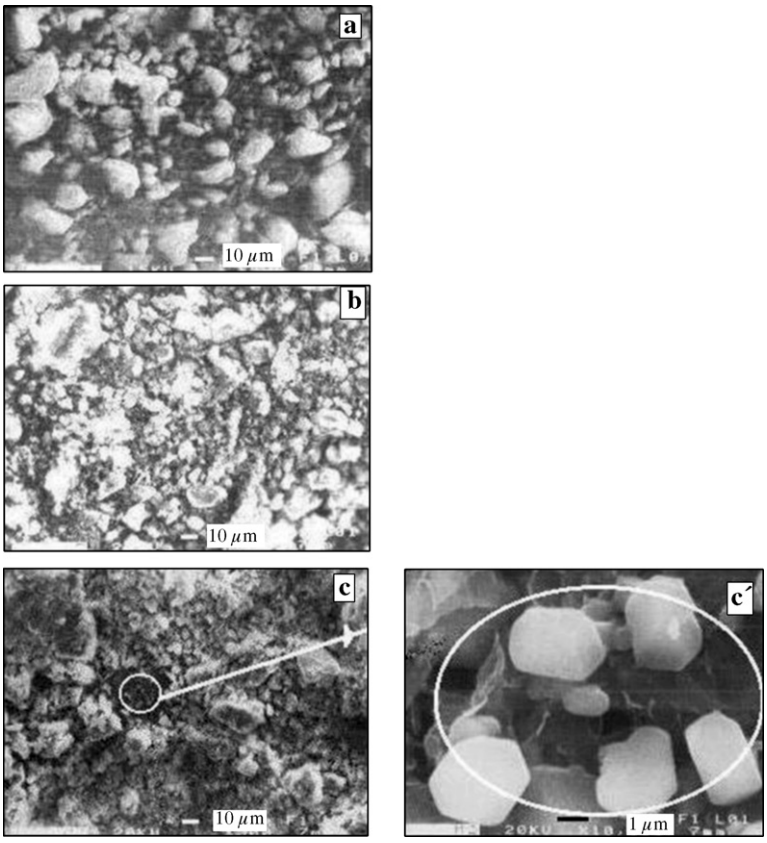

Fig. 4. Electron microscopy photos of samples of initial bentonite clay (a); after addition of NaOH (b); after addition of TMA in samples **b** (c, c′); c′—localization point of $Ca(OH)_2$ crystals.

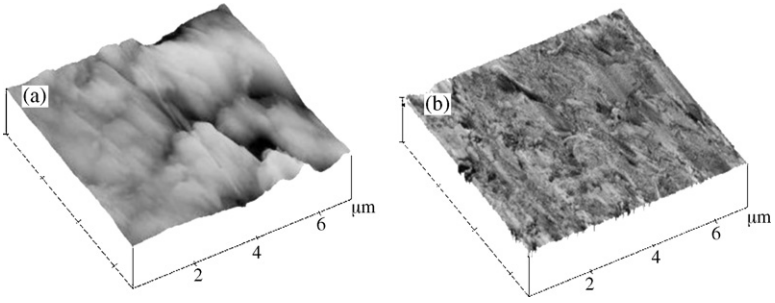

Fig. 5. AFM image of initial bentonite clay in the height (a) and phase (b) regime.

time, AFM images (Fig. 8d) show the formation of a new phase (white color) on edges of smectite flakes. This represents the process of dehydroxylation of smectite [2,5].

At 1452 cm^{-1} a new absorption band attributed to M–OH bonds is observed, where M is Ca, Na, etc. (see Fig. 3b). Based on the X-ray microanalysis data this band can be attributed to $Ca(OH)_2$ [20,21]. Note that in Fig. 4c and c′ $Ca(OH)_2$ occurs in the form of hexagonal micro-crystals. The formation of $Ca(OH)_2$ is possible by the following reaction:

$$CaSO_4{\cdot}2H_2O + 2NaOH \rightarrow Ca(OH)_2 + Na_2SO_4{\cdot}2H_2O.$$

IR bands of absorption in $Ca(OH)_2$ are: 3648, 1427 and 874 cm^{-1}. Superposition of a strong absorption band of $Ca(OH)_2$ with a band of AlAlOH at 3627 cm^{-1}, results in an

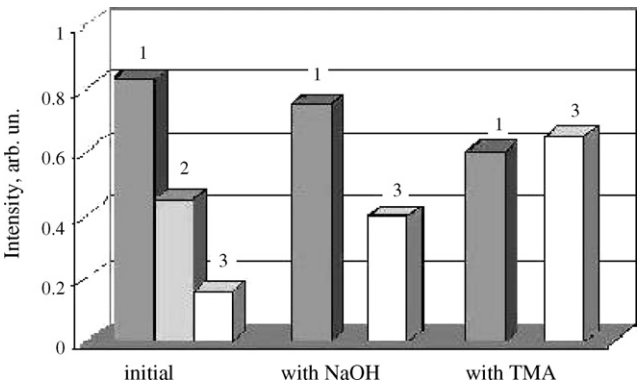

Fig. 6. Change of diffraction line intensity depending on the type of treatment of bentonite clay. Smectite (1), gypsum (2), halo (3).

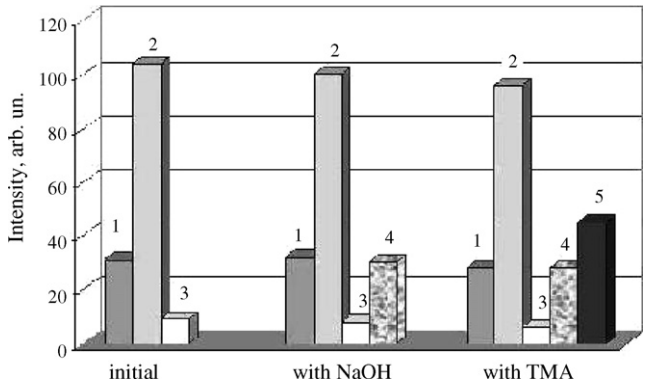

Fig. 7. Change of FTIR line intensity depending on the type of treatment of bentonite clay. For (1) ν∼795.8 cm^{-1} (Si–O of bonds); (2) 466.8 cm^{-1} (Si–O–Al bonds); (3) 842.5 cm^{-1} (Al–Mg–OH bonds); (4) 1423 cm^{-1} (M–OH bonds, where M is Ca); (5) 2853 cm^{-1} (CH-bonds of TMA).

"apparent" increase of intensity of the AlAlOH band. In the region of 1700–1000 cm^{-1} broadening and distortion of the left shoulder of the absorption band of Si–O and Si–O–Si bonds of smectite is marked.

A strong adsorption band of sodium sulfate lies at 1125 cm^{-1} [20,21]. It contributes to the intensity of the absorption band of smectite and causes its distortion. One should note that the strongest lines of sodium sulfate were detected in the solid residue of an evaporated liquid taken from one sample of series **b**.

In due course a high-frequency wing (shoulder) of the absorption band of smectite in the 1600–1000 cm^{-1} region is deformed (reduced). This is attributed to the initial stage of carbonation of calcium hydroxide.

The destruction of smectite aggregates is marked in SEM and AFM images (Figs. 4a, b and 8a, c).

A computer simulation of superimposed spectra was carried out for the analysis of transformations in the observed FTIR-spectrum, into which montmorillonite, gypsum, calcite, cristobalite, quartz, and sulfate of sodium were included [21]. Some of these spectra are represented in Fig. 9.

3.3. Introduction of TMA into activated bentonite (series **c**)

After the introduction of TMA into activated bentonite (into samples **b**) the pH remains high and equal to 11.2. Reduction of the smectite content and an essential increase of the halo are registered (see Figs. 2a, c and 6). The value of the $d_{(001)}$ line is considerably increased (up to 2.811 nm). An additional low-intensity line with a small value of $d_{(001)}$ is observed.

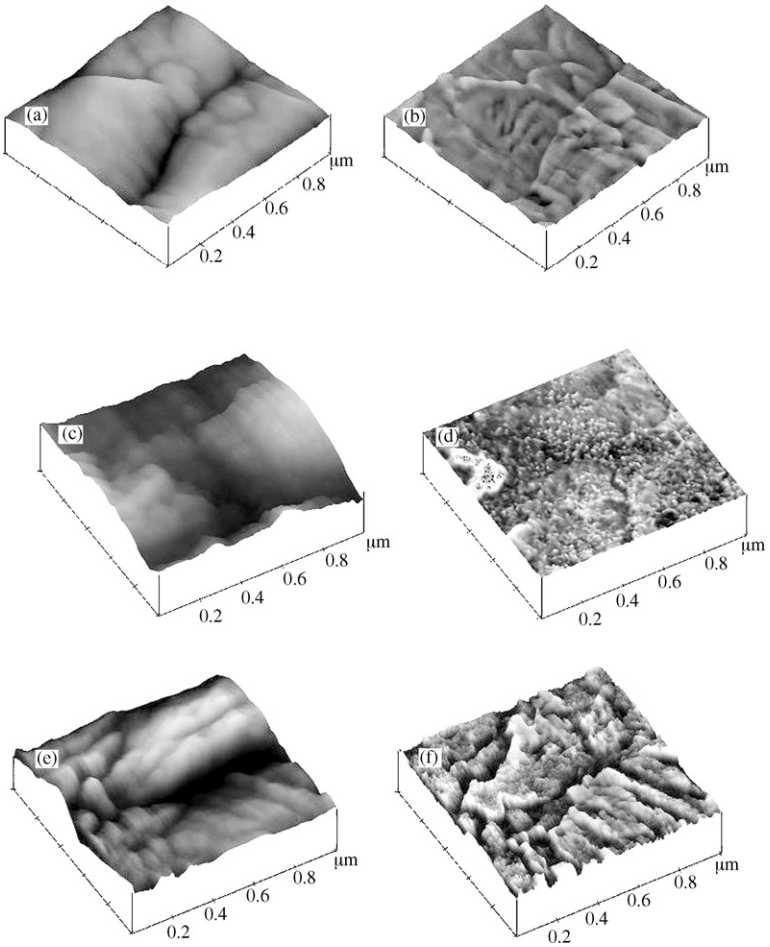

Fig. 8. AFM image of initial bentonite clay (a, b), after NaOH-activation (c, d), after addition of TMA (e, f). (a, c, e) in the height regime and (b, d, f) in the phase regime.

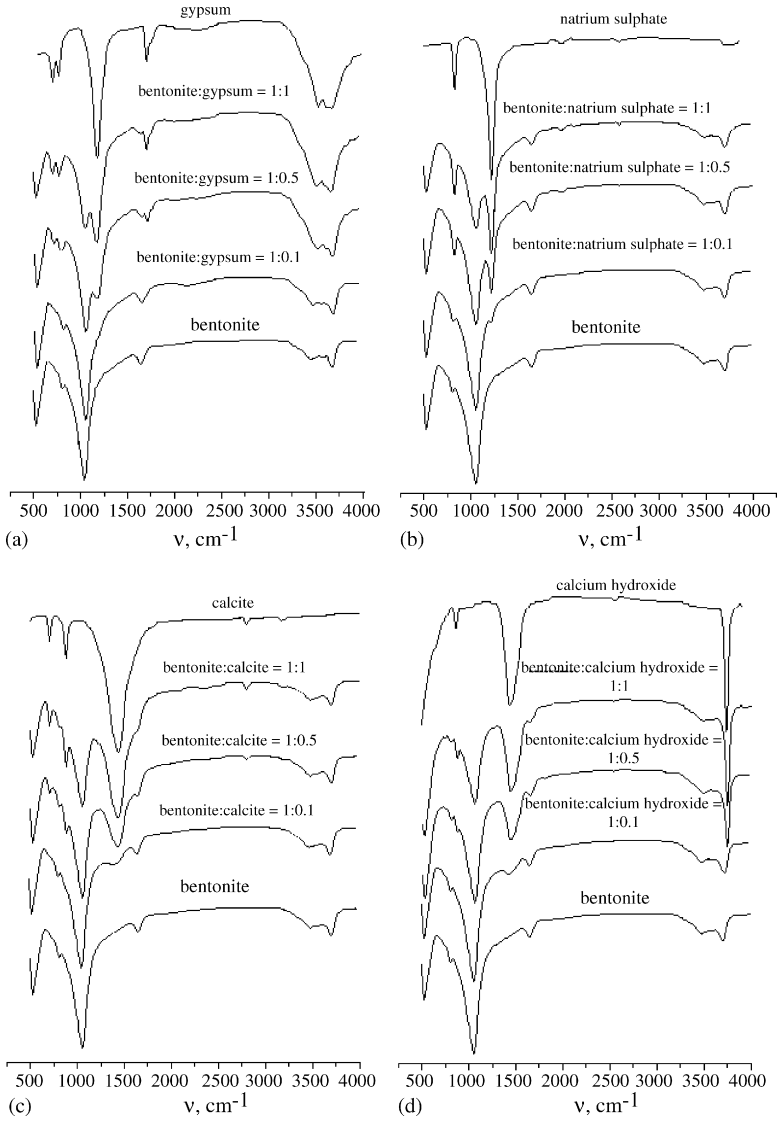

Fig. 9. FTIR superimposed spectra of a binary system (a–d) with different component ratios.

In FTIR-spectrum of smectite an increment of OH-band intensity in the region of 3450 cm^{-1}, and the appearance of new absorption bands, which belong to CH bonds of TMA is observed (see Table 1, Figs. 3c and 7). Widening and distortion of Si–O and Si–O–Si bands of the absorption of smectite in the region of 1600–1000 cm^{-1} is observed. The intensity of bands at $\nu \sim 795$ cm^{-1} (Si–O bonds), 460–520 cm^{-1} (Si–O–Al(Mg) bonds), 920–840 cm^{-1} (AlAlOH and AlMgOH bonds) is less than in initial bentonite clay (see Fig. 7).

Electron microscopy data (Fig. 4c) shows that after addition of TMA the size of smectite aggregates decreases. Crystals of $Ca(OH)_2$ with a hexagonal form are present inside pores among smectite aggregates (Fig. 4c′). Their formation is caused by slow crystallization from a supersaturated solution during evaporation of moisture [22].

In AFM images the destruction of smectite aggregates is more precisely visible (Fig. 8c and e). The phase regime on the edges of smectite flakes represents a more neogenic phase (white color), than in samples of series **b** (Fig. 8d and f). The specific surface is ~ 20 m^2/g. The value of CEC is zero. This means that TMA molecules have exchanged practically all sodium cations.

4. Discussion

This study performed in conditions of water deficiency and its evaporation has enabled an observation of interaction processes of impurities and smectite with an alkaline medium. Thus, a more integral picture of the influence of NaOH and TMA on bentonite can be presented. It includes macro-and micro-transformations in bentonite.

Let us consider macro-transformations. After addition of NaOH the increase of S_{sp}, reduction of aggregate size, essential distortion of a strong band of absorption of smectite in the region 1700–1000 cm^{-1}, the occurrence of a FTIR-band of absorption from $Ca(OH)_2$ testify that destruction of primary aggregates (containing inclusions of gypsum, quartz and cristobalite) and the formation of new compounds occur. The latter are precipitated on the surface of neogenic aggregates

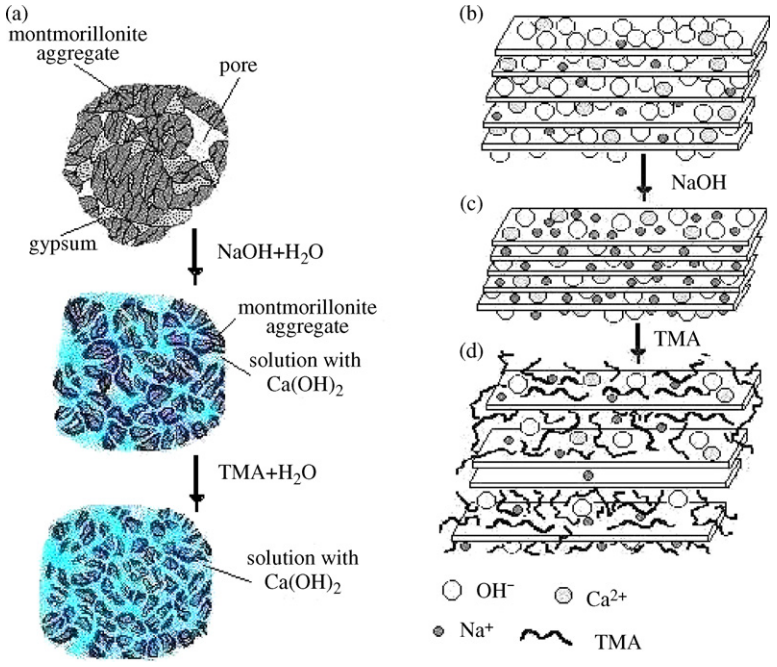

Fig. 10. Macro-reconstruction of bentonite (a) and micro-reconstruction of montmorillonite (b–d) at different treatment stages.

and in pores. First of all, disintegration of aggregates is realized in points of impurity congestion. The process of aggregate destruction slows down after the evaporation of moisture and recommences after the introduction of a new portion of a water solution. Therefore, after the addition of TMA destruction of aggregates accompanied by an S_{sp} increase is observed. However, the calculated specific surface value does not reflect true S_{sp} as neogenic salts, brine and hydrosilicates formed (for example, tobermorite) with cement properties prevent penetration of nitrogen molecules (in the BET method) in pores [23]. Finally, an insignificant increase in Si–O band intensity in **b** samples and its reduction in **c** samples set occurred (see Fig. 7). This process is shown in Fig. 10a.

Let us consider micro-transformations in the smectite lattice.

Reduction of $d_{(001)}$ to 1.243 nm after the addition of NaOH, coupled by changes in the FTIR band intensity of interlayer water, reflects the introduction of Na cations into interlayer space forming Na-smectite. A single water interlayer complex forms in the interlayer space instead of a double water interlayer complex, which is inherent for Ca-, Ma-smectite [1,2,11,12,24,25].

The increase of $d_{(001)}$ (X-ray data), significant diminution of CEC, and increase of ''water'' bands into interlayer space (FTIR data) after the addition of TMA is explained by displacement of Na-water complexes from interlayer space of smectite and its saturation with organic cations [2,24,26]. It is possible that after addition of TMA an inorganic-organic-clay formed (if Na is present in smectite particles) [12,27,28].

Low values of $d_{(001)}$ (''collapsed'' interlayers) are characteristic for saturated interlayer space with polyvalent cations and a non-uniform distribution [2,15,24,25]. This process is shown in Fig. 10b.

Detection of CH-bands in FTIR-spectra specifies adsorption of TMA molecules on the surface of smectite aggregates-particles (see Fig. 3). It may be one of the reasons causing weakening of absorption band intensity at 795, 460–520 and 920–840 cm^{-1} and the increase of the crystallogram halo. As AFM images denote formation of a new phase on smectite edges, it is possible that these places can be zones of calcium hydrosilicate initiation based on the formation of SiO_2 [23] due to dehydroxilation of smectite.

As a high pH is maintained in **b** samples, destruction of smectite aggregates and partial dissolution of the mineral take place after the addition of new water portions (after addition of a water solution of TMA, **c** samples) [10,26]. Dehydroxilation of smectite, in our opinion, is the consequence of a pH increase during moisture evaporation moisture from a sample (especially in a porous one).

We shall note that frequently there are divergences when a comparison of qualitative and semi-quantitative X-ray and FTIR analysis is made. It is caused by a number of reasons. One of them is only an implementation error. During spectra recording with a high speed or short time of integration (Figs. 2 and 3) it is difficult to notice minor alterations of line intensity (area under the line). Mostly, line amplitudes are compared. However, for slow spectra recording or short time of integration when line intensities (areas) are compared minor changes in phases contents are easily registered (Figs. 6 and 7).

5. Conclusions

Within the framework of a uniform cycle an investigation is carried out of some directions in the development of bentonite transformations:

1. Introduction of a NaOH solution in bentonite initiates destruction of large aggregates of bentonite due to interactions of the alkali with accessory phases.
2. The interaction of gypsum with NaOH in a water solution converts Na, Ca-smectite into Na-smectite accompanied by the formation of Na–H_2O complexes, instead of Ca–$2H_2O$ complexes.
3. Addition of TMA leads to: (a) replacement of Na–H_2O complexes by organic molecules into interlayer space; (b) covering of the surface of smectite particles by a layer of TMA molecules.
4. Conditions of water deficiency and water evaporation promote preservation of a high pH and development of a dehydroxylation process after the addition of new portions of water.
5. Application of semi-quantitative X-ray and IR-methods of investigation enables monitoring of structural-phase transformations in a clay mineral with a greater precision than qualitative methods.

References

[1] H. Van Olphen, Introduction to Clay Colloid Chemistry, John Wiley & Sons, New York-London-Sydney-Toronto, 1977.
[2] H. Kodama, A.R. Mermut, J.K. Torrance (Eds.), Clay for our Future, ICC97 Organizing Committee, Ottawa, Ontario, Canada, 1997.
[3] J.J. Fripiat (Ed.), Advanced Techniques for Clay Mineral Analysis, Elsevier, Amsterdam, 1982.
[4] L. Wang, R. Govind, R.A. Dobbs, Sorption of toxic organic compounds on wastewater solids: mechanism and modelling, Environ. Sci. Technol. 27 (1993) 152–158.
[5] G.E. Christidis, P.W. Scott, A.D. Dunham, Acid Activation, Bleaching capacity of bentonites from the Islands of Milos and Chios, Aegean, Greece, Appl. Clay Sci. 12 (1997) 329–347.
[6] D.W. Rutheford, C.T. Chiou, D.D. Eberl, Effects of exchanges cation the microporosity of montmorillonite, Clays Clay Mineral 45 (1997) 534–535.
[7] L. Heller-Kallai, I. Rosenson, Nontronite after acid or alkali attack, Chem. Geol. 32 (1981) 95–102.
[8] F.R. Valenzuela Díaz, P. de Souza Santos, Studies on the acid activation of Brazilian smectitic clays, Quimica Nova 24 (2001) 345–353.
[9] L. Calarge, B. Lanson, A. Meunier, M.L. Formoso, The smectitic minerals in a bentonite deposit from Melo (Uruguay), Clay Mineral 38 (2003) 25–34.
[10] F. Claret, A. Bauer, T. Schafer, L. Griffault, B. Lanson, Experimental investigation of clays with high-pH solutions: a case study from the Callovo-Oxfordian formation, meuse-haute marne underground laboratory (France), Clay Mineral 50 (5) (2002) 633–646.
[11] P. Komadel, Chemically modified smectites, Clay Mineral 38 (2003) 127–138.
[12] R.M. Barrer, Zeolites and Clay Minerals as Sorbents and Molecular Sieves, Academic Press, London, 1978.
[13] S.A. Boyd, S. Shaobai, J.-F. Lee, M.M. Mortland, Pentachlorophenol adsorption by organo-clays, Clays Clay Mineral 36 (2) (1988) 125–130.
[14] J.-F. Lee, M.M. Mortland, C.T. Chiou, D.E. Kile, S.A. Boyd, Adsorption of benzene, toluene, and xylene by two tetramethylammonium smectites having different charge densities, Clay Clay Mineral 38 (2) (1990) 113.
[15] S. Yariv, Adsorption of organic cationic dyes by smectite minerals, in: Proceedings of second Mediterranean Clay Meeting, vol. 1, 1998, pp. 99–127.
[16] S.K. Dentel, A.I. Jamrah, D.L. Sparks, Sorption and cosorption of 1.2.4-trichlorobenzene and tannic acid by organo-clays, Water Res. 32 (12) (1998) 3689–3697.
[17] S. Yariv, H. Cross (Eds.), Organo-Clay Complexes and Interaction, Marcel Dekker, New York, 2002.
[18] C.I. Rich, Removal of excess salt in cation exchange capacity determination, Soil Sci. 93 (1963) 87–94.
[19] R.H. Okazaki, H.W. Smith, C.D. Moodie, Hydrolysis and salt-retention errors in conventional cation-exchange capacity procedures, Soil Sci. 96 (1963) 205–209.
[20] K. Nacamoto, Infrared Spectra of Inorganic and Coordinated Compounds, Wiley, New York, 1970.
[21] Data Base of FTIR-spectra, 2000. http://www.chem.uni-postdam.de/tools/index.html.
[22] H. Hartman, W. Wegener, Beitrag zum Loschverhalten von Weisskalk in Abhangigkeit von Brenntemperatur und chemischer Zusammensetzung, Zement-Kalk-Gips 6 (1954) 229.
[23] D. Savage, D. Noy, M. Mihara, Modeling the interaction of bentonite with hyperalkaline fluids, Appl. Geochem. 17 (2002) 207–223.
[24] L.P. Meier, R. Nuesch, The lower cation exchange capacity limit of montmorillonite, J. Colloid Interf. Sci. 217 (1999) 77–85.
[25] P. Bala, B.K. Samantaray, S.K. Srivastava, Dehydration transformation in Ca-montmorillonite, Bull. Mater. Sci. 23 (2000) 61–67.
[26] S.M. Mohnot, J.H. Bae, W.L. Foley, A study of alkali/mineral reactions, SPE Reserv. Eng. (1987) 653–663.
[27] K.R. Srinivasan, H.S. Fogler, Use of inorgano-organo-clay in the removal of priority pollutants from industrial wastewaters: structural aspects, Clay Clay Mineral 38 (1990) 277–286.
[28] K.R. Srinivasan, H.S. Fogler, Use of inorgano-organo-clay in the removal of priority pollutants from industrial wastewaters: adsorption of benzo (a) pyrene and chlorophenols from aqueous solutions, Clay Clay Mineral 38 (1990) 287–293.